Torus Constraints of ANEPD-CXO245: A Compton-thick AGN with Double-Peaked Narrow Lines

Martín Herrera-Endoqui[1], Takamitsu Miyaji[1], Mirko Krumpe[2], Masaki Hanzawa[3], Ayano Shogaki[3], Shuji Matsuura[3], Atsushi Tanimoto[4], Yoshihiro Ueda[4], AKARI NEP Deep Field Team

[1]Instituto de Astronomía, sede Ensenada, UNAM, México • [2]Leibniz Institut für Astrophysik, Potsdam, Germany

[3]Department of Physics, Kwansei Gakuin University, Japan • [4]Department of Astronomy, Kyoto University, Japan

Abstract

We constrain the torus parameters of the Compton Thick (CT) AGN ANEPD-CXO245 (z=0.449), which shows double-peaked optical narrow line region (NLR) emission lines, located in the AKARI NEP Deep Field. We analyze the X-ray spectra, obtained with Chandra using the X-ray clumpy torus model XCLUMPY by Tanimoto+2019, and the UV-optical-IR SED, including the unique AKARI nine-band photometry over 2-24 μm, using our implementation of the model CLUMPY by Nenkova+2008 in the package CIGALE (Noll+2009; Boquien+2019). With the combination of these analyses we are able to constrain the torus optical depth, X-ray absorbing column, torus angular width, and viewing angle. The results show that the line of sight crosses the torus, as expected for type 2 AGN. Comparing the optical depth of the torus from the UV-Optical-IR SED and the absorbing column density NH from the X-ray spectrum, we find that the gas-to-dust ratio is about 8 times larger than the Galactic value.

Introduction and motivation

Doble peaked narrow line regions appear in about 1% of the present-day type 2 AGN (Liu+2010). They can be caused by dual AGN, wind driven outflows, radio-jet driven outflows and rotating ring-like NLR (Müller-Sánchez +2015). Knowing the geometrical parameters of the torus can help to discriminate among some of these scenarios, particularly between the outflow and rotating ring-like NLR: if the opening angle of the torus is narrow, it is more difficult for a rotating ring-like NLR to cross the ionization cone and this scenario would be unlikely. On the other hand, if the line of sight is almost perpendicular to the polar axis, the two sides of the bipolar outflow should show similar line-of-sight velocities and this scenario would be unlikely. This also tells us something about the evolutionary stage of CT-AGN, since they can be at the stage of starting feedback through outflows or tidally-disrupted in-falling clouds generating a ring-like structure.

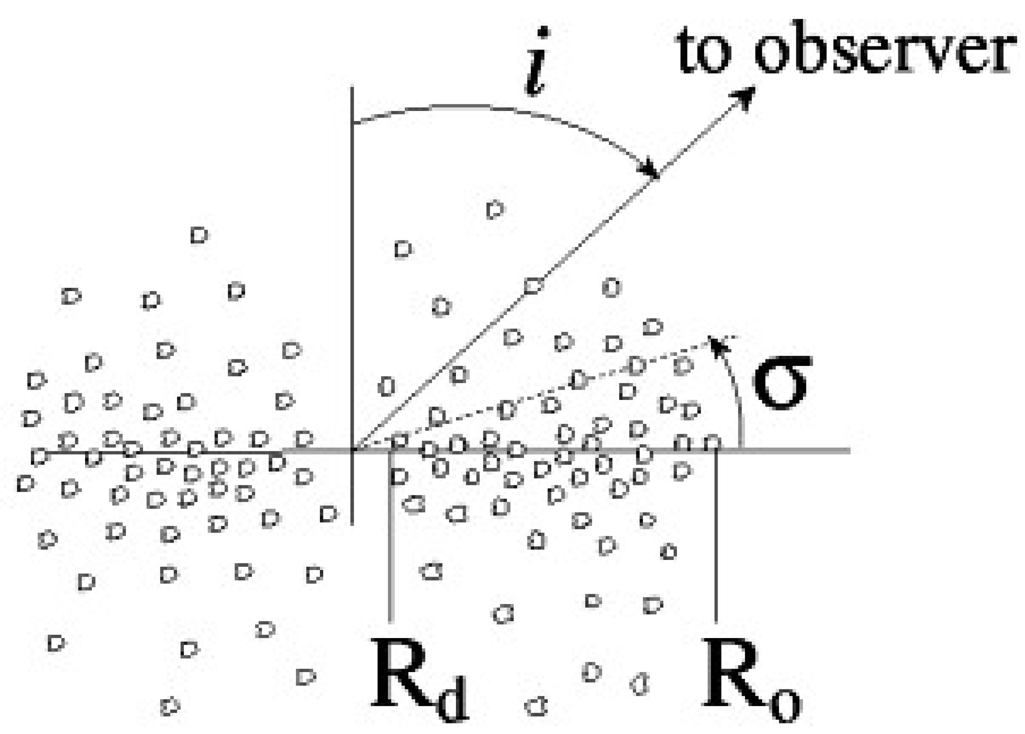

Modern AGN torus models (like the one shown above; Nenkova+2008), both in the infrared and X-rays, have opened up the possibility of constraining its geometric parameters such as the torus angular width (σ) and the viewing angle (*i*), in addition to the optical depth and the X-ray absorption column density. In this work we analyze the X-ray spectrum and the UV-optical-IR SED in order to discriminate between the bi-polar flow and the rotating ring-like NLR scenarios, by finding the geometrical parameters of the AGN torus.

Data

We combine information from our multi-wavelength survey on the AKARI NEP Deep Field (ANEP) where deep observations with all the nine bands of the InfraRed Camera (IRC; λ eff = 2,3,4,7,9,11,15,18 & 24 μm) were made, including Chandra X-ray observations (Krumpe+2015; Miyaji+2017), optical spectroscopy (Shogaki 2018) and UV-optical-infrared SED analysis (Hanami+2012) for the object ANEPD-CXO245. This object was found as a result of our AKARI survey on the North Ecliptic Pole (NEP) region (AKARI NEP Deep Field; e.g. Matsuhara+2006).

UV-Optical-IR (UOI) data.

We use UOI photometric measurements from GALEX (Burgarella+2019), Subaru Telescope Suprime Cam (SCAM) (Murata+2013), Canda-France-Hawaii Telescope (CFHT) MegaCam and WIRCAM (Oi+2014), and Herschel PACS (Pearson+2019)/SPIRE (Pearson+, in prep).

X-ray data and reduction.

A major fraction (∼ 0.25 deg^2) of ANEPD has been observed with Chandra with a total exposure of ∼ 300ks (Krumpe+2015). ANEPD-CXO245 is covered by the Chandra ACIS-I FOVs of seven OBSIDs (total exposure ∼ 120 ks). The X-ray spectrum of each OBSID has been extracted using standard tools of Ciao[1]. A combined spectrum is created along with appropriately weighted mean response matrix and a background.

Analysis and results

Optical spectrum

The KECK DEIMOS spectrum of ANEPD-CXO245 in rest frame. The fluxes of each emission line have been obtained with Gaussian+linear continuum fits. We observe, among other things, that the profiles of [OIII]λ5007 in the radial velocity space is well represented by two narrow and a broader components (insert). Other profiles ([NeIII]λ3869 and [NeV]λ3425) show similar double peaks. The star-formation dominated line [OII]λ3727 is single-peaked. Our nominal redshift (z = 0.499) is based on this line.

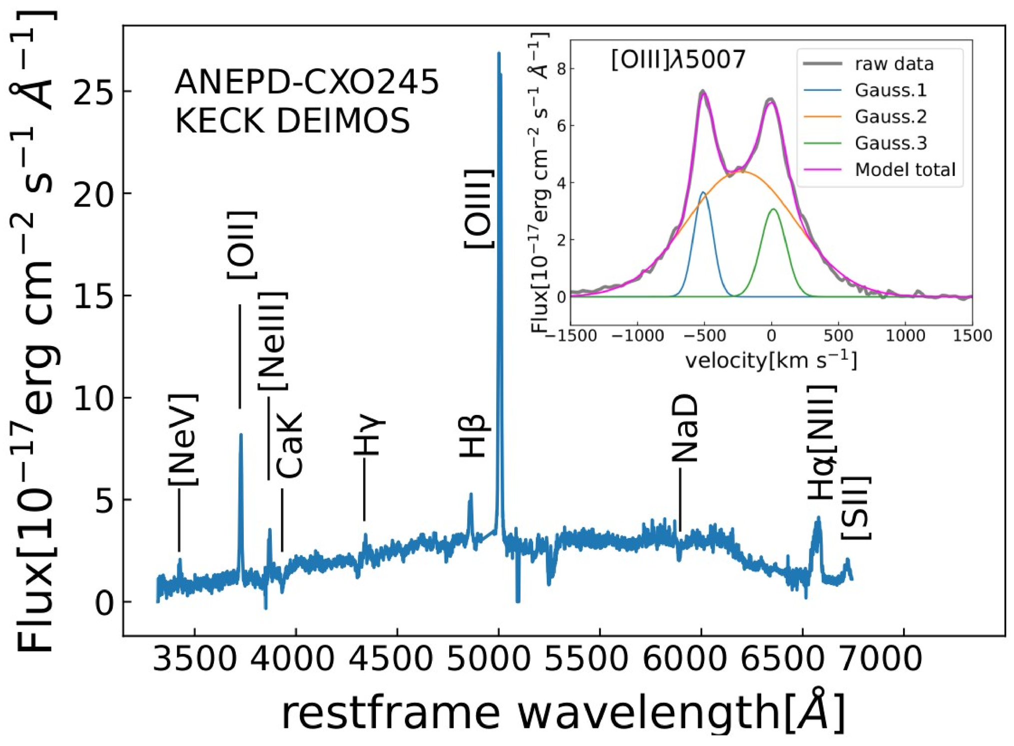

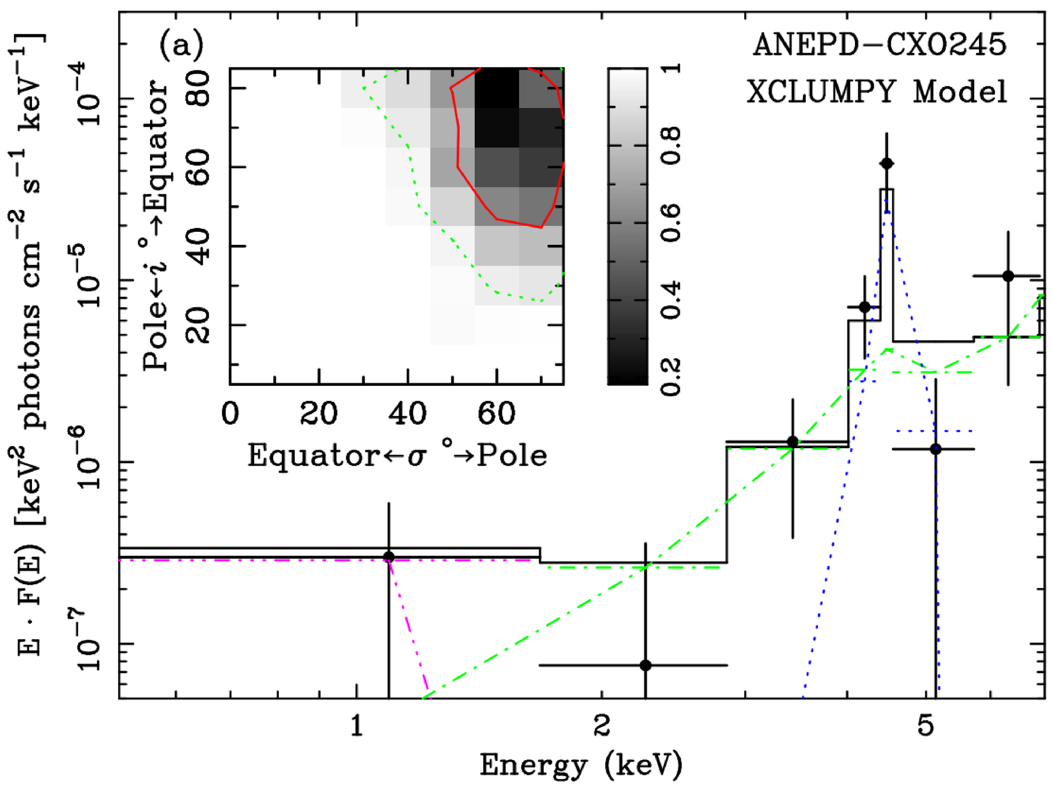

X-ray spectrum

Chandra spectrum of ANEPD-CXO245. The spectrum is analized with XSPEC[2] using the new X-ray Clumpy Torus model XCLUMPY (Tanimoto+2019). Shown are the best-fit model and the contribution of various components. Also shown is the integrated probability grayscale image and its 68% and 95% contours. The spectrum shows a strong Fe Kα line characteristic of a CT-AGN.

We find that NH ≥ 6 10^{24} cm^{-2}, thus this object can be classified as CT-AGN, and values of 90° − *i* ≥ σ, meaning that the line of sight crosses the torus material, as expected for type 2 AGN with a lower limit to the viewing angle (*i* > 36°)

UOI SED

UV-Optical-IR SED (≈ 0.2 − 1000 μm) of ANEPD-CXO245 obtained with our implementation of the clumpy torus model CLUMPY[3] (Nenkova+2008) into the CIGALE[4] package (Noll+2009; Boquien+2019). We search for the best fit parameters assuming values consistent with the current version of XCLUMPY. The insert represents the integrated probability grayscale for the parameter space σ - *i*, and the 68% and 95% confidence levels.

We find that the values of log($L_{IR,AGN}$) and $\tau_V N_0$ are well constrained (values are 44.6 and 400, respectively). log($L_{IR,AGN}$) changes very little when we use other models of torus and the star formation dust components (Fritz+2006; Schreiber+2016).

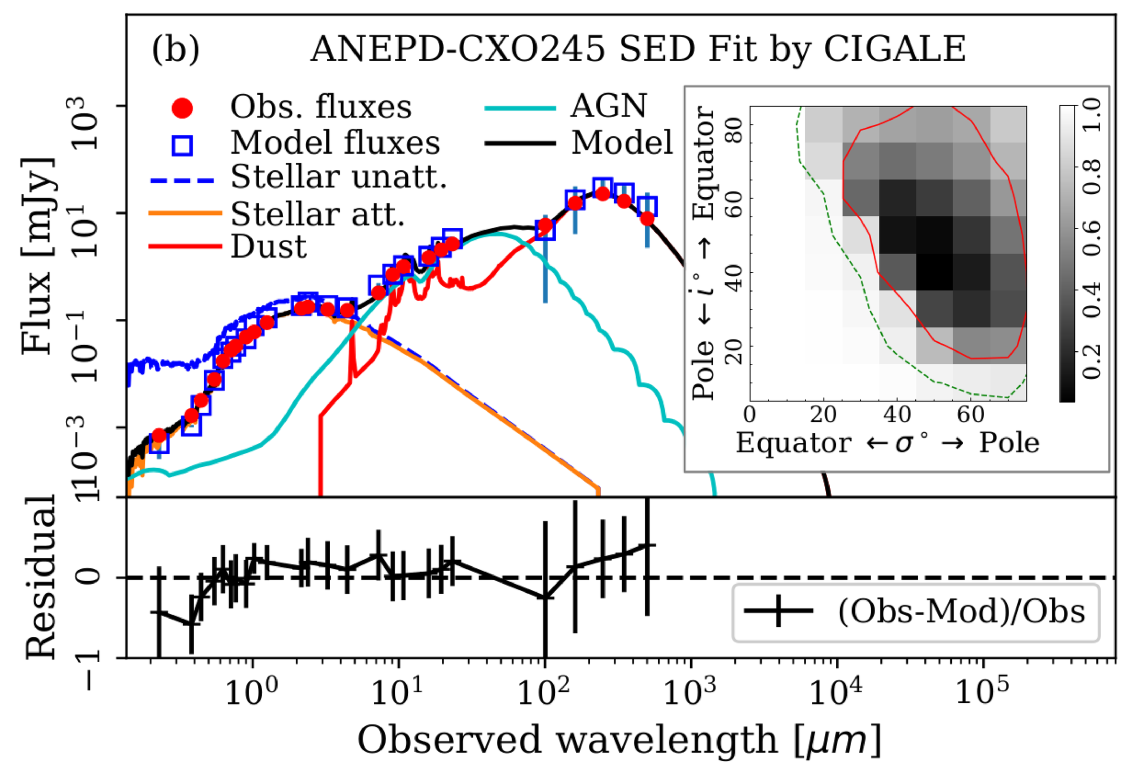

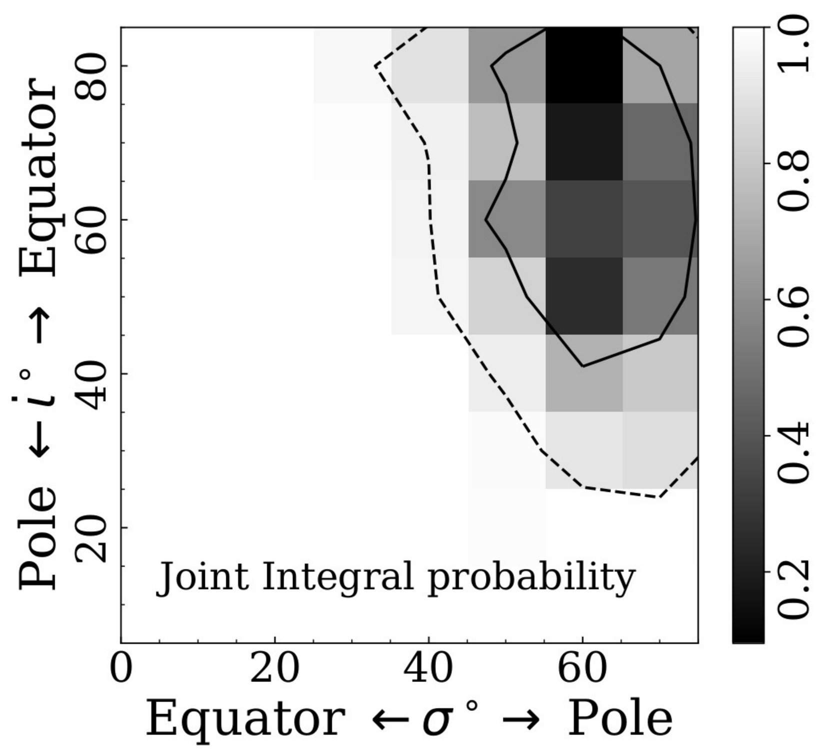

Combining the obtained values of NH from the X-Ray analysis and $\tau_V N_0$ from the IR analysis we find N_H^{Equ}/A_V^{Equ} ≥ 8 × 10^{21} cm^{-2} mag^{-1}, while the Galactic value is N_H/A_V = 1.87 × 10^{21} cm^{-2} mag^{-1} (Draine 2003). This implies that the gas-to-dust ratio in the torus of ANEPD-CXO245 is at least 8 times larger than that of our Galaxy, which is consistent with the results from e.g. Tanimoto+2019, who have found a gas-to-dust ratio of ∼ 26 times the Galactic value for the nearby CT-AGN the Circinus galaxy.

X-Ray and IR Joint Torus constraints

The joint integrated probability map calculated for the joint constraints of the torus parameters that are common to both XCLUMPY and CLUMPY (σ and *i*) show that the preferred values are those in which the line of sight crosses the torus.

Future prospects

The Wide Field Imager (WFI) on the future Advanced Telescope for High Energy Astrophysics (Athena)[5] is expected to be able to obtain a useful spectrum of this object up to the rest frame energy of ∼ 20 keV, tracing some of its Compton hump in the continuum. A preliminary spectral simulation shows that a 100 ks WFI observation of this object would be able to constrain σ (*i*) to approximately ±10° (20°) (90% confidence) level. The Mid-Infrared Instrument (MIRI) on board the James Webb Space Telescope (JWST) would allow us to obtain a continuous spectrum of this object in 5 ≤ λ [μm] ≤ 25 with at least 10σ per wavelength pixel resolution even with a < 10 ks of exposure in each configuration[6] (Glasse+2015) and would tighten constraints on the dust torus parameters.

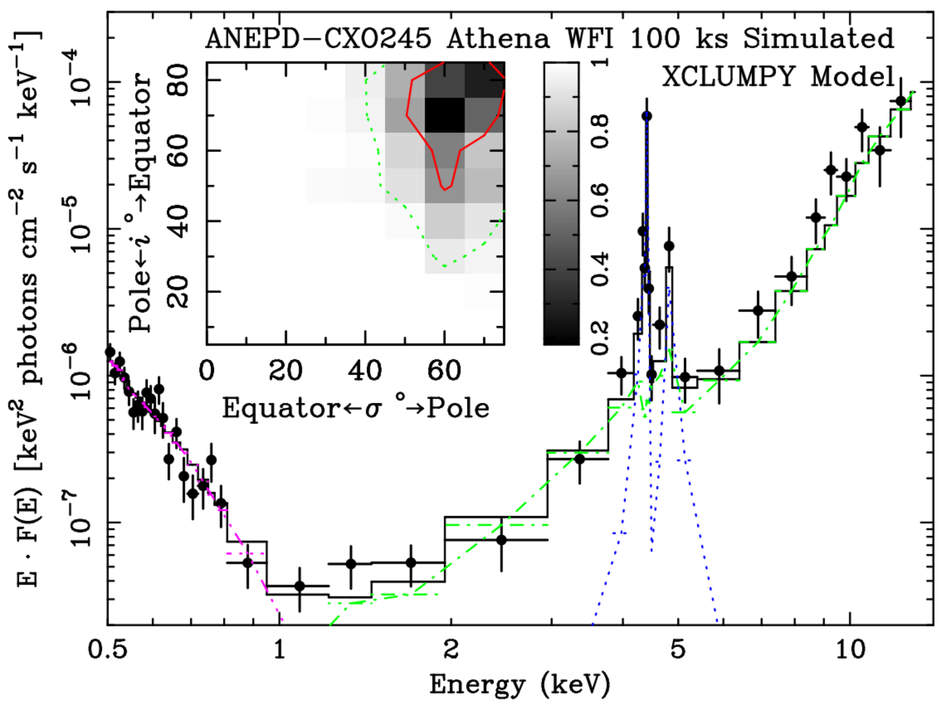

The authors akcnowledge financial support from PAPIIT IN111319 and CONACyT 252531.

References

[1]http://cxc.harvard.edu/ciao • [2]https://heasarc.gsfc.nasa.gov/ • [3]https://www.clumpy.org/ • [4]http://www.the-athena-x-ray-observatory.eu/ • [5]https://cigale.lam.fr • [6]http://www.stsci.edu/jwst/science-planning/

Liu, X., Shen, Y., Strauss, M. A., & Greene, J. E. 2010, ApJ, 708, 427
Müller-Sánchez, F., Comerford, J. M., Nevin, R., et al. 2015, ApJ, 813, 103
Nenkova, M., Sirocky, M. M., Ivezić, Ž., et al. 2008, ApJ, 685, 147
Krumpe, M., Miyaji, T., Brunner, H., et al. 2015, MNRAS, 446, 911
Tanimoto, A., Ueda, Y., Odaka, H., et al. 2019, ApJ, 877, 95
Fritz, J., Franceschini, A., & Hatziminaoglou, E. 2006, MNRAS, 366, 767
Miyaji, T., Krumpe, M., Brunner, H., et al. 2017, Publication of Korean Astronomical Society, 32, 235
Shogaki, A., Master Thesis, Kwansei Gakuin University (in Japanese)
Hanami, H., Ishigaki, T., Fujishiro, N., et al. 2012, PASJ, 64, 70
Matsuhara, H., Wada, T., Matsuura, S., et al. 2006, PASJ, 58, 673
Noll, S., Burgarella, D., Giovannoli, E., et al. 2009, A&A, 507, 1793
Schreiber, C., Elbaz, D., Pannella, M., et al. 2016, A&A, 589, A35
Burgarella, D., Mazyed, F., Oi, N., et al. 2019, PASJ, 71, 12
Murata, K., Matsuhara, H., Wada, T., et al. 2013, A&A, 559, A132
Oi, N., Matsuhara, H., Murata, K., et al. 2014, A&A, 566, A60
Pearson, C., Barrufet, L., Campos Varillas, M. d. C., et al. 2019, PASJ, 71, 13
Boquien, M., Burgarella, D., Roehlly, Y., et al. 2019, A&A, 622, A103